remote sensing

MDPI

Supplementary 1: GIA in Himalaya

Global calculation of is GIA based on various proxies namely, sea level changes **(Peltier 1999),** visco-elastic model **(Wahr et al. 2000),** a combination of ice loading history and visco-elastic model **(A et al. 2016).** There have been many attempts to define GIA in Himalaya **(Wang 2001)** or effectively isolate GIA from Hydrology **(Xiang et al. 2016).** Our approach is to make use of existing models to demonstrate the effect of GIA in Himalaya- Tibet region on the seasonal to decadal hydrological and glaciological changes in our study area i.e. HGR as shown in Figure A1. The relative merits and demerits of these GIA models not discussed, rather the effect of each of these models on EOF modes of HGR is stressed, since the paper deals with analysis of EOFs of the mascon solution rather than the solution itself. GIA for the broader region surrounding HGR is calculated from three prevalent models namely ICE-6G: **Stuhne and Peltier 2015, Peltier 2004**, (Figure A1.a) and CDGIA: **Wahr et al. 2000,** Figure A1.c, and the GIA corrections provided by CSR based on **A et al. (2016),** Figure A1.b. ICE-6G and CDGIA are essentially global models, which are constrained to Himalaya and surrounding area (Figure A1). The range of GIA from each of these models is under 3mm/yr which is miniscule compared to the trend of mascon solutions for this area which is $\pm$ 5 cm/yr. There is a spatial consistency in the relative magnitude, although ICE-6g and CDGIA which are models at finer resolution show subtle patterns. GIA provided by CSR is removed from the mascon solutions (named raw mascon for convenience) and EOF is calculated. GIA correction from each of the models is applied to the mascons followed by EOF calculation and compared with the EOFs of raw mascons. The results are tabulated in TableA1. GIA correction has no influence on the major EOF modes, as seen in Table 1. The GIA effect on surface mass changes in HGR is too small to be statistically significant in EOF analysis.

Table 1.

	Raw mascons (GIA correction not applied)	**GIA- corrected ICE-6G**	**GIA- corrected CSR**	**GIA- corrected Wahr 2000**
Number of major modes	6	6	6	6
Covariance of first mode	64.53%	64.53%	64.53%	64.53%
Mutual correlation- GIA corrected vs RAW mascons		0.99	0.98	0.99

a

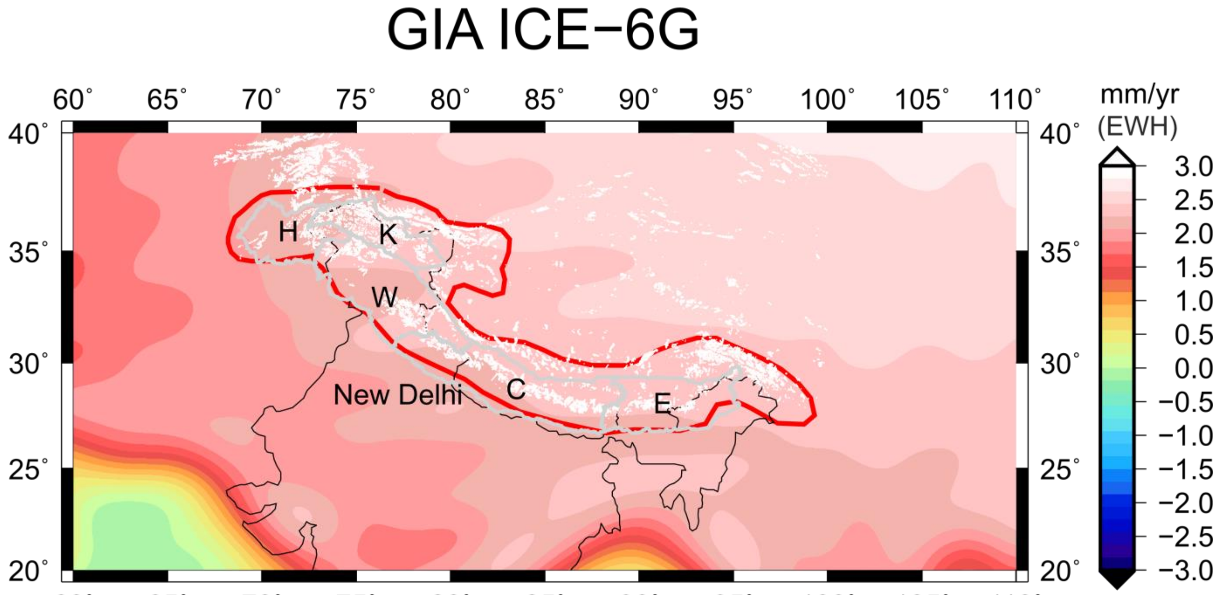
GIA ICE−6G
60° 65° 70° 75° 80° 85° 90° 95° 100° 105° 110°
40° 35° 30° 25° 20°
H
K
W
New Delhi
C
E
mm/yr
(EWH)
3.0 2.5 2.0 1.5 1.0 0.5 0.0 −0.5 −1.0 −1.5 −2.0 −2.5 −3.0

b

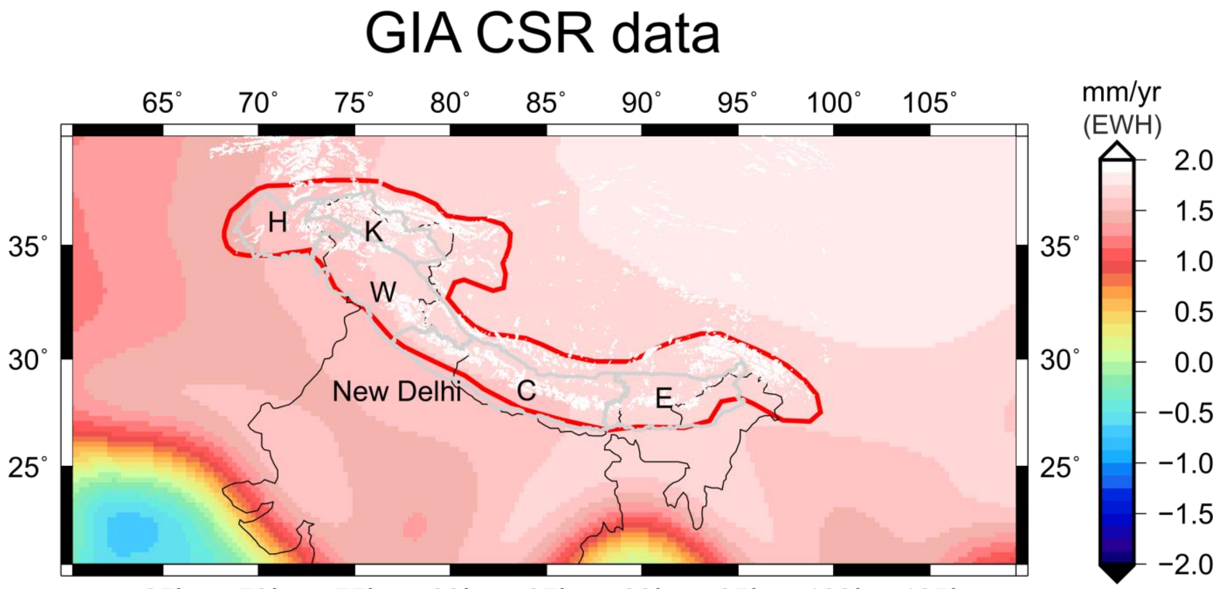
GIA CSR data
65° 70° 75° 80° 85° 90° 95° 100° 105°
35° 30° 25°
H
K
W
New Delhi
C
E
mm/yr
(EWH)
2.0 1.5 1.0 0.5 0.0 −0.5 −1.0 −1.5 −2.0

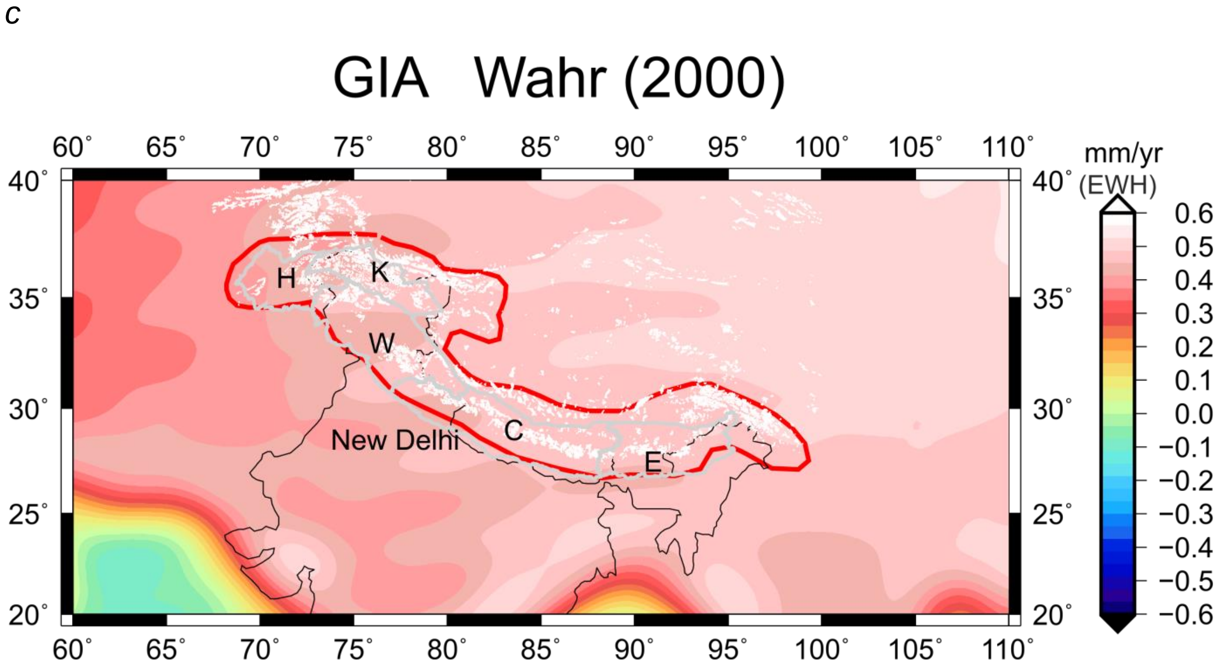

Figure 1. GIA calculated from models and CSR given grids (a) ICE - 6G model (b) CSR-mascon (c) Wahr 2000 model.

Reference:

1. A Geruo, Wahr J., and Zhong S. (2013), Computations of the viscoelastic response of a 3-D compressible earth to surface loading: An application to glacial isostatic adjustment in Antarctica and Canada, Geophys. J. Int., 192(2), 557–572, doi:10.1093/gji/ggs030.
2. Preltier.W.R(1999) Global sea level rise and global isostatic adjustment. Global and Planetary Change 20 _1999. 93–123
3. Peltier. W.R., (2004). Global Glacial Isostasy and the Surface of the Ice-Age Earth: The ICE-5G (VM2) Model and GRACE, Ann. Rev. Earth and Planet. Sci., 32, 111-149.
4. Stuhne,G.R., Peltier.W.R. (2015) Reconciling the ICE-6G_C reconstruction of glacial chronology with ice sheet dynamics: The cases of Greenland and Antarctica. J. Geophys. Res. Earth Surf. 120, 1-25, doi:10.1002/2015JF003580.
5. Wahr John, Wingham Duncan, Bentely Charles (2000) A method of combining ICESat and GRACE satellite data to constrain Antarctic mass balance. Journal Of Geophysical Research, Vol. 105, No. B7, Pages 16,279-16,294, July 10, 2000
6. Wang Hansheng (2001) Effects of Glacial isostatic adjustment since the late Pleistocene on the uplift of Tibetan Plateau. GJI 144, 448-458
7. Xiang Longwei, Wang Hansheng, Steffen Holger, Wu Patrick, Jia Lulu, Jiang Liming, Shen Qiang(2016). Groundwater storage changes in the Tibetan Plateau and adjacent areas revealed from GRACE satellite gravity data. Earth and Planetary Science Letters 449 (2016) 228–239. http://dx.doi.org/10.1016/j.epsl.2016.06.002

Supplementary 2: External influences:

Lesser modes up to 1% of variance i.e. modes 2 to 4 of the interannual TWS, are analysed similar to the first mode i.e. correlation and causality analysis of the modes with climatic variables i.e. precipitation, snow accumulation in water equivalents and air temperature. The lesser modes are analysed fully although they contribute very small part to the variance because modes up to 1% variance contribution are statistically significant i.e. they are not error. Spatial patterns of each of these modes show that centre of influence i.e. the place where anomaly originated is outside the study area.

Second highest contribution of ~8 % is shown on mode 2 (Fig A2.a), this mode shows an increasing trend in the time series. The spatial variation implies the division of the area into three regions, positive western and eastern end and negative central parts. However, the centres of mass change are outside Himalaya for this mode. This mode does not correlate with climatic variables. For the eastern and central part, the centre of influence is located in the river basin at the foot hills of the Himalaya and for the western end the centre of influence is to the north of the Himalaya.

In case of the third mode (Figure A2.b), the spatial pattern comprises of smaller localized features again whose centres are outside the study region. This mode contributes only 3% of the total variance, weight of this signal is not significant. Also, a very weak correlation with climatic variables i.e. <0.25 is registerd.

Mode 4(Figure A2.c), strikes as the part of GRACE signal containing interference of Ganga basin as -ve centre is located at the lower end of the spatial plot, near to Ganga basin. Lagged correlation of mode 4 with precipitation over Himalaya, SWE and groundwater levels over Ganga basin, is done. None of the above variables show any significant correlation i.e. less than to +0.4 all at lag zero with the mode. Causality analysis results are not significant. Based on visual interpretation it is deduced that, the centre of Ganga basin low, located approximately 400 Km away from the Himalayan boundary, causes a perturbation of 1% in the seasonal removed total mason variation as captured by this mode.

Gathering the spatial patterns and temporal evidences together, mode2 shows the external perturbation influence on mass variation, depicts smaller locally significant mass variation and mode4 depicts the extent of influence of Ganga basin low over Himalayan region, i.e. the part of Himalaya signal perturbed by Ganga Basin influence. Hence, the lesser modes depict the mass perturbation in HGR which do not pertain to the glaciology in HGR. By extension, the first mode solely represents HGR glaciology, without any influence from external factors including the Ganga basin perturbation.

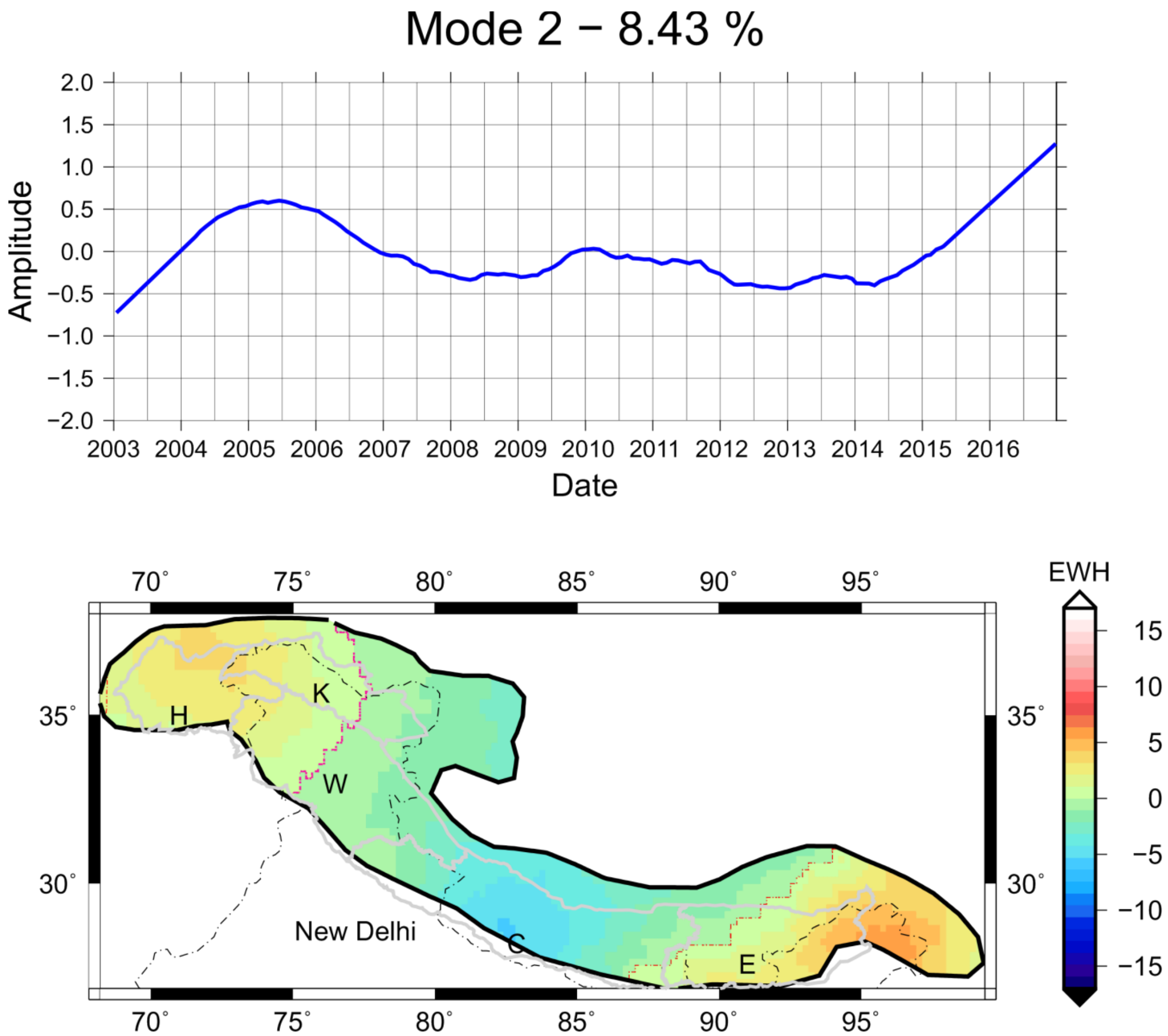
Mode 2 − 8.43 %
Amplitude
Date
2.0
1.5
1.0
0.5
0.0
−0.5
−1.0
−1.5
−2.0
2003
2004
2005
2006
2007
2008
2009
2010
2011
2012
2013
2014
2015
2016
70°
75°
80°
85°
90°
95°
35°
30°
H
K
W
New Delhi
C
E
EWH
15
10
5
0
−5
−10
−15

a

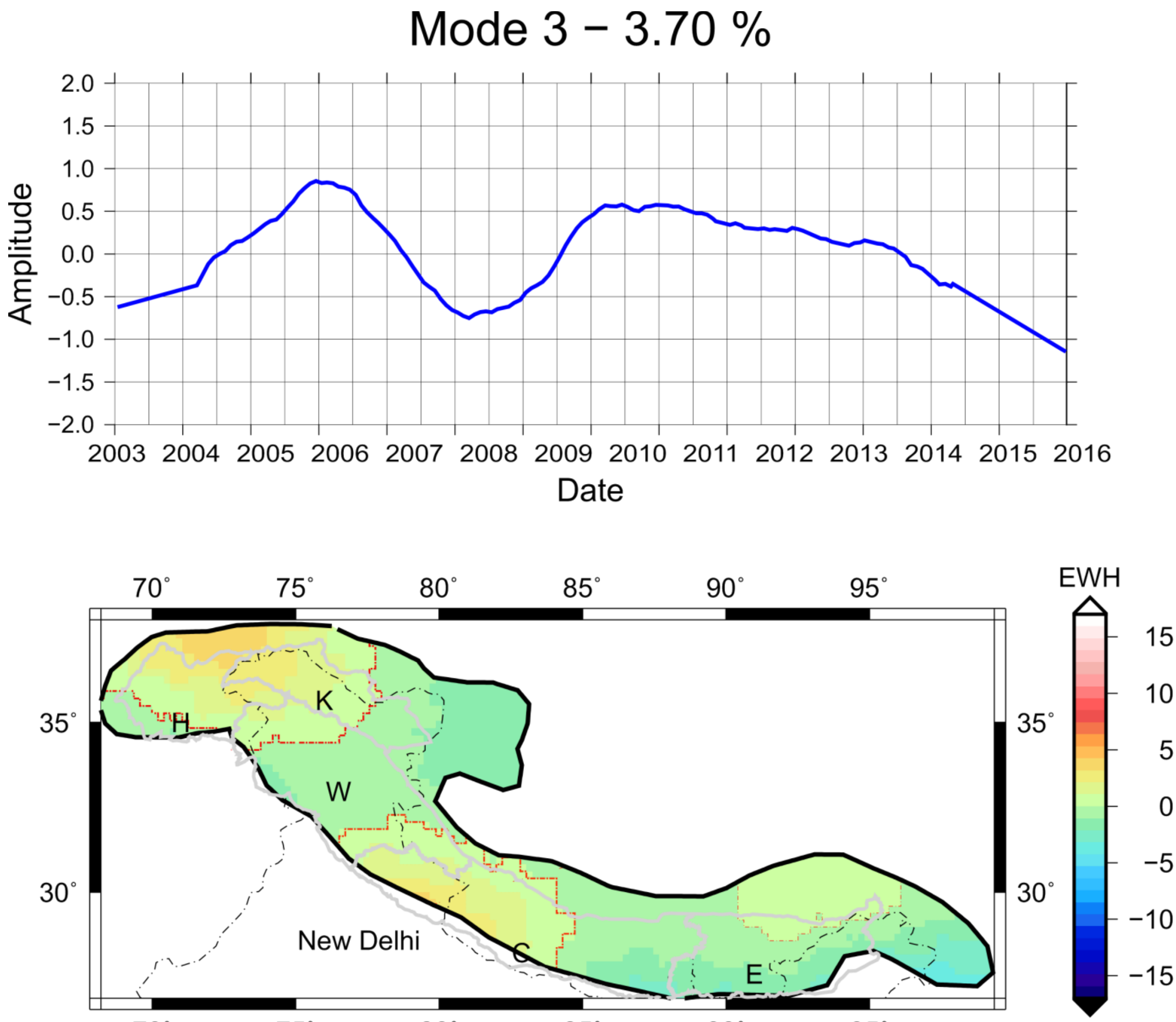
Mode 3 − 3.70 %
Amplitude
Date
2.0
1.5
1.0
0.5
0.0
−0.5
−1.0
−1.5
−2.0
2003
2004
2005
2006
2007
2008
2009
2010
2011
2012
2013
2014
2015
2016
70°
75°
80°
85°
90°
95°
35°
30°
H
K
W
C
E
New Delhi
EWH
15
10
5
0
−5
−10
−15

b

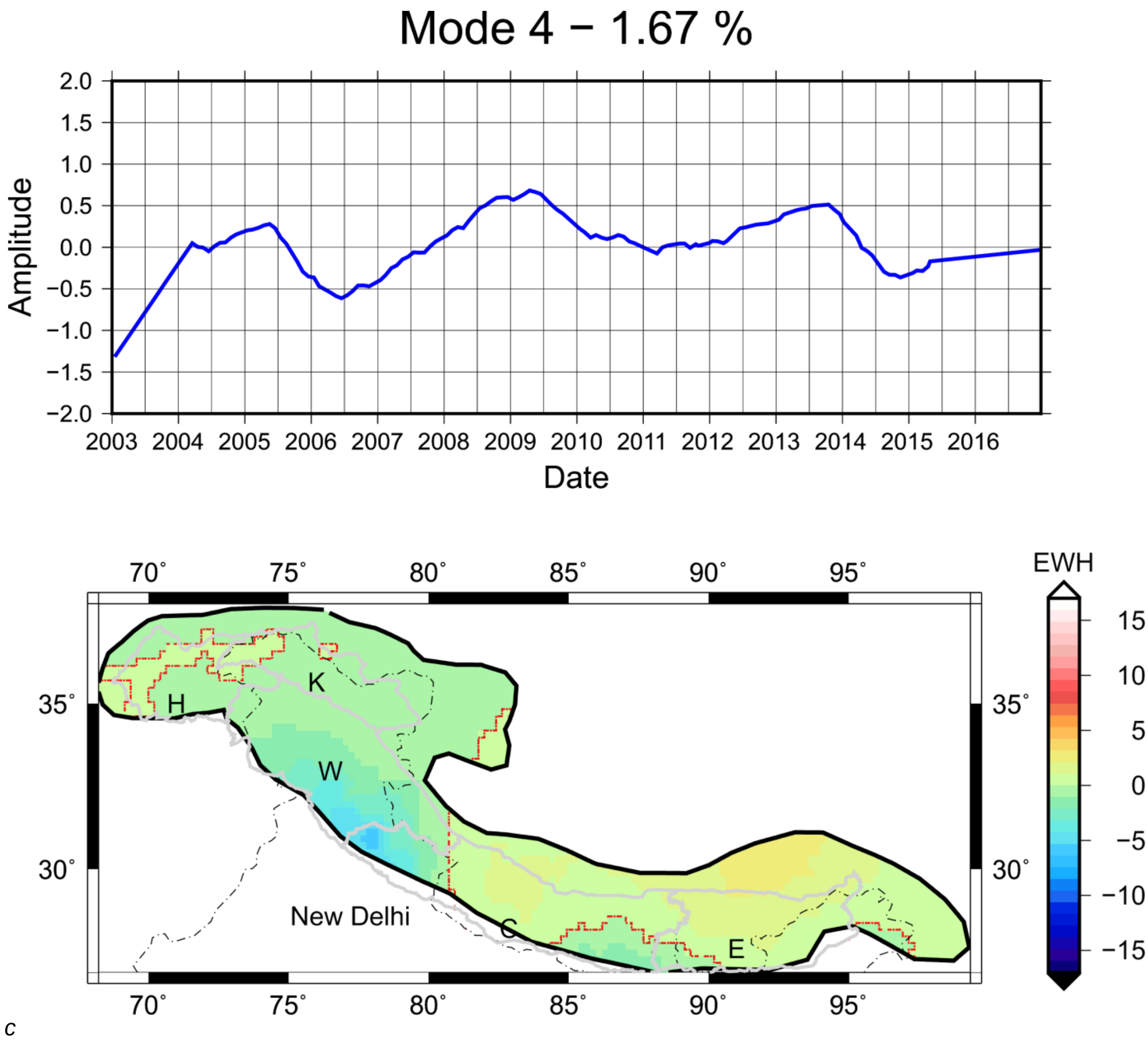

Figure 2. GRACE - lesser modes of Himalaya at seasonal removed time scale a. Mode2 b. Mode3 c. Mode4.